Materials Research Proceedings 41 (2024) 977-982 https://doi.org/10.21741/9781644903131-107

The non-proportional loading of mild steel

HAZRA Sumit[1,a *], DHARA Sisir[1,b], TAYLOR Scott[1,c] and FIGIEL Łukasz[1,d]

[1] WMG, University of Warwick, Coventry, CV4 7AL, UK

[a]sumit.hazra@warwick.ac.uk, [b]Sisir.Dhara.2@warwick.ac.uk, [c]Scott.Taylor.1@warwick.ac.uk, [d]L.W.Figiel@warwick.ac.uk

Keywords: Strain Path Change, In-Situ Microstructure Evaluations, Formability

Abstract. The effect of proportional loading on formability has been extensively studied. However, non-proportional loading occurs frequently in a stamping operation and its impact on formability has been studied less. Non-proportional loading occurs in two areas of stamping: continuously during the draw stage of a complex geometry and discontinuously through stamping stages. Studies on non-proportionality (eg. [1]) show that it can change the formability of a material compared to when it is loaded proportionally. This paper introduces an experimental method that allows a comparison of the deformation in mild steel subject to continuous and discontinuous loading mechanisms. A notable innovation of the method is that it can be carried out inside the chamber of a scanning electron microscope, allowing in-situ measurements of plastic deformation. The experiments show that the plastic behavior of the material under the continuous mode is distinct to when it is deformed discontinuously

Introduction

Automotive stamping is a multi-stage process. In the first, drawing stage, the material is drawn over a complex tool to undergo the majority of its final deformation. In follow-on stages, the drawn component is allowed to springback and then may be processed in follow-on steps to produce the final geometry. This process results in continuous and discontinuous strain path change mechanisms. The continuous mechanism takes place during the draw stage when the material flows over complex geometry of the draw tool, which forces the strain path of the material to change when the material encounters transitions in geometry. The discontinuous mechanism occurs when the component is removed from the draw tooling, allowing it to springback and is subsequently deformed along a different strain path when it is re-drawn or flanged in a following stage.

The current experimental state-of-the-art has focused on the effects of the discontinuous mechanism on formability. Dhara et al. [1] simulated the discontinuous mechanism in an AA5754-O aluminum alloy by first pre-straining samples uniaxially in a tensile machine and subsequently re-loading along the biaxial strain path using a miniature Nakajima test. They found considerable increase in the subsequent forming limits of the material. More recently, Collins et al. [2] observed a similar phenomenon in low carbon ferritic steel samples. Using a purpose-built tester, cruciform samples were first pre-strained along a uniaxial strain path, unloaded and then loaded biaxially. They found a significant increase in the limit strains.

The effect of the continuous mechanism has not been studied as thoroughly as the discontinuous mechanism. Song et al. [3] and Leotoing and Guines [4] developed a complex cruciform specimen to change its strain path continuously from uniaxial to biaxial tension using a sophisticated servo-hydraulic testing machine. They found that continuously mechanism caused changes to the forming limit strains in steel (DP600) and aluminum (AA5086) but they did not contrast the changes to that produced by the discontinuous mechanism. Hence, an important contribution was made by Yoshida et al. [5] and Yoshida and Kuwabara [6], who compared the continuous and discontinuous mechanisms in stress space. They made three findings. First, the stress-based

characterization of forming limits was path independent when the strain path change was discontinuous. Second, the limit stress was path dependent when it was continuous. Third, path-dependent nature was directly affected by the strain hardening behavior of the material. Erinosho et al. [7, 8] showed that strain hardening behavior is related to the orientation of grains in the microstructure and the evolution of dislocation density during the discontinuous mechanism.

To investigate the relationship between the externally applied loading and microstructural deformation, in-situ deformation techniques are increasingly used. During an in-situ test, a material is elongated using a micromechanical test rig that is placed in a scanning electron microscope (SEM) chamber. The deformation of the material can be evaluated using secondary electron or electron back-scatter diffraction detectors to image and measure textural changes respectively. For example, Ghadbeigi et al. [9] and Celotto et al. [10] deformed dual-phase 1000 (DP1000) steel and transformation induced plasticity 800 (TRIP800) steel samples uniaxially using a miniaturized loading rig. They captured SEM images of the sample surface and post-processed the images using the digital image correlation (DIC) technique to analyze the evolution of strain distribution in the ferritic and martensitic phases of their specimens.

In this work, the in-situ technique was adapted to investigate the effect of continuous and discontinuous mechanisms on its microstructural deformation. Tests were performed on DX54 in the uniaxial and then biaxial strain paths. A novel sample geometry was designed to enable the material to be deformed continuously and discontinuously. Using DIC, strains were measured at the macroscale and the microscale. The results showed that the material deformed differently at the macroscale and this was reflected in the microstructural deformation of the material.

Method

A Micromecha Proxima test rig was used to perform the strain path change experiment (Fig.1). The rig was placed in a Zeiss Sigma SEM and was controlled with Micromecha's POROS 2 software. The 'inline' and 'transverse' grips of the rig are connected through a 45° wedge. The rig's motor pulls inline grip 1 and its motion is translated into a perpendicular motion to load the transverse grips via the wedge connection. The peak capacity of the rig is 3.5kN. Load and extension were captured by sensors on the rig and recorded to the POROS 2 software in real time. Displacement was applied to the inline grip 1 at a rate of 5µm/sec and the test was interrupted every 0.2mm to image the microstructure. Images were captured using a 10keV voltage source and a secondary electron detector.

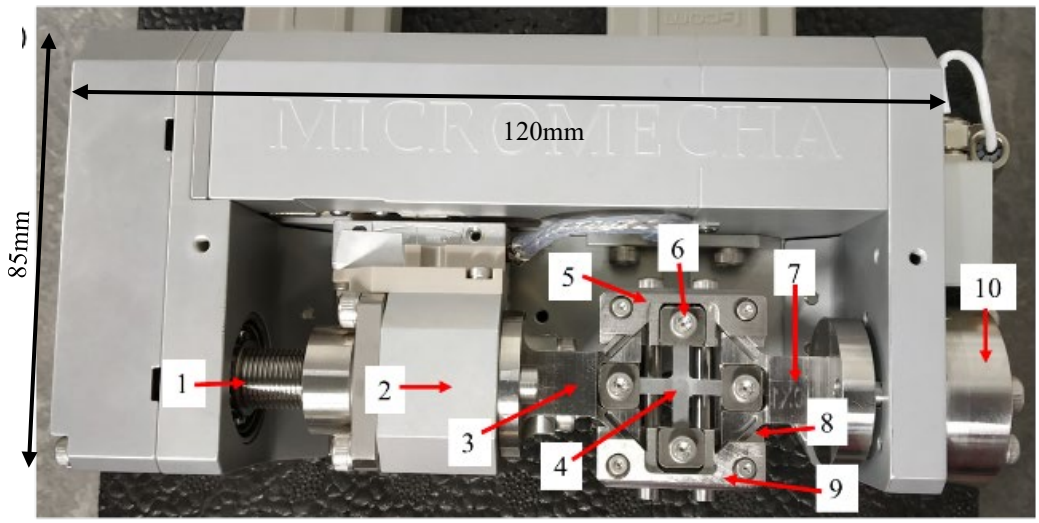

Fig.1 Top view of the Micromecha Proxima rig. 1: Lead screw, 2: Motor, 3: In-line grip 1, 4: Specimen, 5: Transverse grip 1, 6: Connecting bolt, 7: In-line grip 2, 8: 45° wedge, 9: Transverse grip 2, 10: Load cell

The 30 x 30mm cruciform sample design proposed by Caër and Pesci [11] was used for the tests. To perform the continuous tests, 30 x 30mm sample was modified to include 0.2mm length slots in the transverse arms of the sample (Fig.1, component 6). The slots were added to allow the connecting bolts of the transverse grips (Fig.1, component 1 and 9) to translate without loading the specimen at the start of the test. When the connecting bolts reached the end of the slots, it loaded the transverse arms of the specimen to load the sample biaxially. In this way, the material was deformed uniaxially until 0.108 strain, then loaded biaxially until failure. The discontinuous tests were carried out by loading the cruciform sample uniaxially until 0.108 strain by simply disconnecting the transverse grips. The sample was then unloaded to fix the transverse grips, then reloaded biaxially until failure. The key difference between the discontinuous and continuous modes is the unloading step in the discontinuous mode.

The deformation of the material was measured at the macroscopic and microscopic scales. At the macroscopic scale, the strain evolution was measured with a GOM 12M DIC system. The DIC system consisted of two 12MP cameras fitted with 75mm lenses. A paint speckled paint pattern was applied to the sample surface before the test and GOM ARAMIS version 6.1 software was used to acquire and process the captured images to calculate strain contour [12]. Length resolution was 0.36mm and measurement uncertainty of the system was measured to be ±0.0006 [13].

To measure microstrains, the deformation of the sample was captured in a Zeiss Sigma SEM and its images post-processed with LaVision's DIC software (DaVis 10) [13]. The samples were polished and etched with 2% Nital solution for 10s to reveal the microstructural features within the microstructure. The image of the microstructure was captured every 200µm of deformation. Using the manufacturer recommended subset size of 25pixels and step size of 8pixels (to give length resolution of 13µm), the features in the evolving microstructure was tracked by the DIC software to estimate the strain within the microstructure. Displacement accuracy of the system was 0.01 pixels, which corresponded to a strain resolution of about ±0.001 strains [13].

The mechanical properties of the DX54 steel used in these experiments were measured with tensile tests and are shown in Table 1.

Table1 Mechanical properties of DX54

Material		DX54
Gauge [mm]		1
Thickness of central thinned region [mm]		0.3
Young modulus [GPa]		213
Yield strength [MPa]		225
Ultimate tensile strength [MPa]		329
Elongation [strain]		0.43
Anisotropy parameters	r_0	1.53
	r_{45}	1.08
	r_{90}	2.16
Hardening parameters according to Hollomon law	Strength coefficient, K [MPa]	555
	Hardening exponent, n	0.20

Results and discussion

The macroscopic deformation in strain space is shown in Fig.2, which compares the deformation of material undergoing discontinuous (red line) and continuous loading (blue line). Point A is the start of the deformation, point B is the abrupt transition from uniaxial to biaxial deformation and points C and C' are the failure points for the continuous and discontinuous tests respectively. As expected, the initial uniaxial strain path was identical for both loading conditions and the point of the strain path change occurred within 0.002 major strain. There are two key differences in the subsequent biaxial stage. First, the strain ratios ($\varepsilon_{xx}/\varepsilon_{yy}$) were 0.78 ± 0.04 for continuous loading and 0.97 ± 0.03 for the discontinuous loading, an approximately 0.19 difference in strain ratio. Secondly, the elongation of the discontinuous strain path change was found to be consistently higher (by about 0.07 major strain) than the continuous tests.

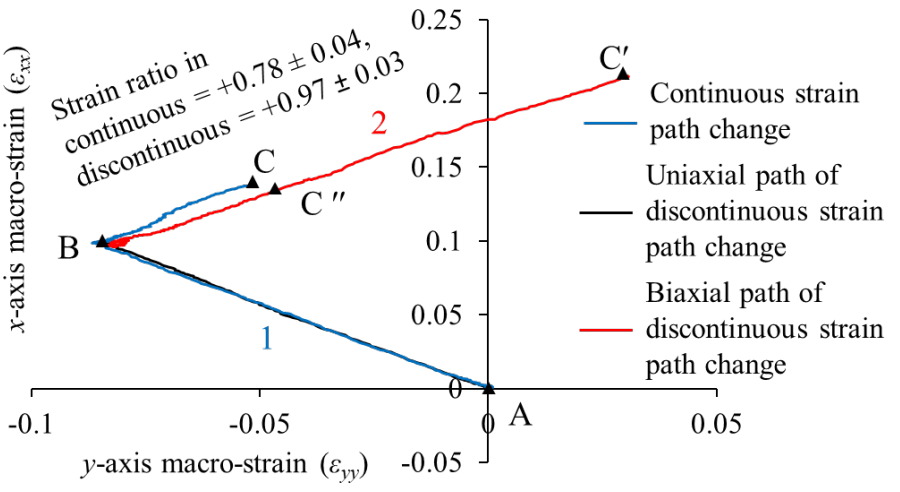

Fig 2 Deformation of continuous and discontinuous strain path change in strain space

At the microscale, the applied deformation on the sample coincided with a heterogeneous of strain in the microstructure (Fig.3). Fig.3a shows strain distribution for the continuous loading and Fig.3b shows strain distribution for discontinuous loading. The strain path change occurred at 1000µm displacement and this corresponded to point B in Fig.2. For the discontinuous tests, the strain path change involved unloading the sample at 1000µm and then re-loading along the biaxial path (Fig.3b). Two observations can be made. First, the heterogeneous strain distribution had a banded

structure and these bands tended to remain consistent during each deformation path. Second, the continuous and discontinuous loadings can be distinguished by the change to this banded structure after the strain path change. During the uniaxial loading, the banded structure started vertically and gradually inclined about 35° to the *x*-axis for both the continuous and discontinuous loadings. After the strain path change, the banded structure in the continuous samples increased slightly to 36° until failure. In the discontinuous strain path change, the 35° banded structure that was observed during uniaxial deformation was replaced by a banded structure that was vertical and remained vertical until failure.

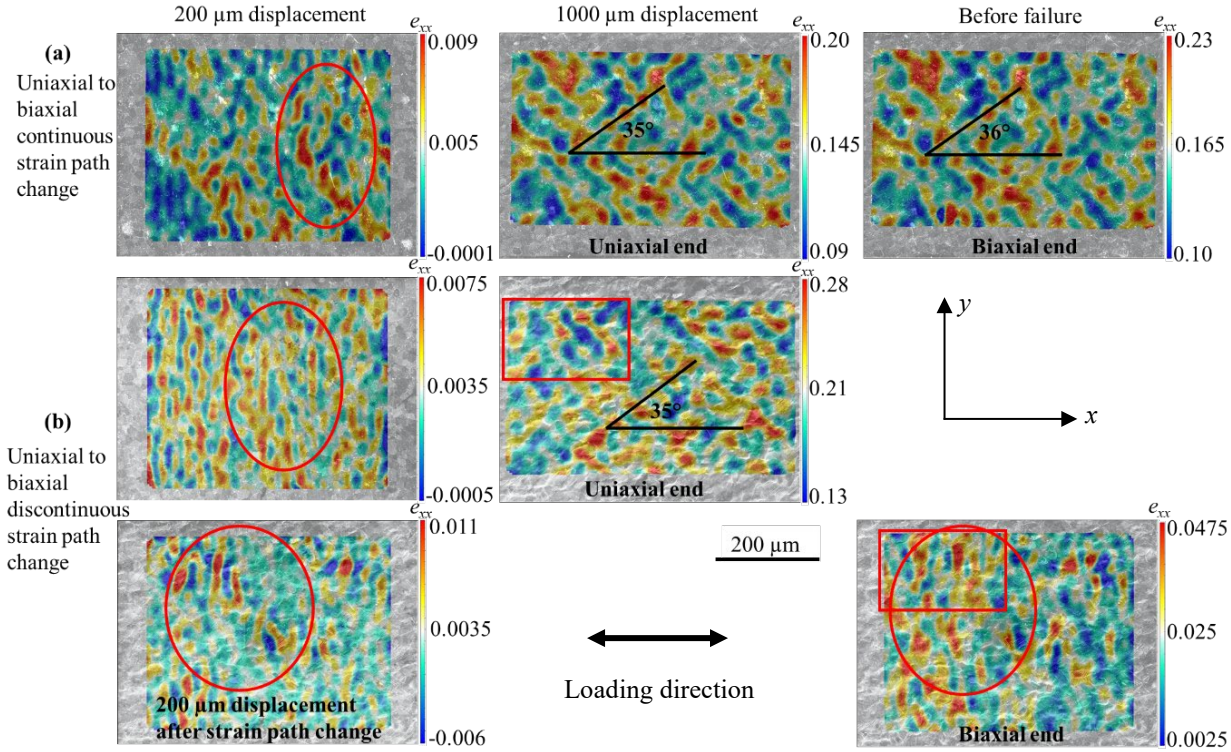

Fig.3 x-axis micro-strain (ε_{xx}) distribution. Left column: 200µm displacement, middle column: 1000µm displacement, right column: before failure, (a) row: continuous loading, (b) row: discontinuous loading. Strain path change occurs at 1000µm

Summary

Stamping is a complex process that involves continuous and discontinuous non-proportional loading of material. To address the gap in understanding of material under non-proportional loadings, an experiment was developed and carried out to evaluate deformation behavior of DX54 under continuous and discontinuous loading from the uniaxial to biaxial strain paths.

In-situ experiments were carried out on cruciform samples that were loaded by a mechanical rig that was small enough to fit in the chamber of a scanning electron microscope. This allowed the deformation of the material to be studied under macro and micro-scales. A comparison of results of the macro and micro scales showed that differences in macroscale behavior are reflected in the microstructural behavior of the material.

References

[1] S Dhara, S Basak, SK Panda, S Hazra, B Shollock, R Dashwood, Formability analysis of pre-strained AA5754-O sheet metal using Yld96 plasticity theory: Role of amount and direction of uni-axial pre-strain, J Manuf Process 24 (2016) 270–82. https://doi.org/https://doi.org/10.1016/j.jmapro.2016.09.014

[2] DM Collins, T Erinosho, FPE Dunne, RI Todd, T Connolley, M Mostafavi, A synchrotron X-ray diffraction study of non-proportional strain-path effects, Acta Mater 124 (2017) 290–304. https://doi.org/https://doi.org/10.1016/j.actamat.2016.11.011

[3] X Song, L Leotoing, D Guines, E Ragneau, Effect of continuous strain path changes on forming limit strains of DP600, Strain 55 (2019), e12329. https://doi.org/https://doi.org/10.1111/str.12329

[4] L Leotoing, D Guines, Investigations of the effect of strain path changes on forming limit curves using an in-plane biaxial tensile test, Int J Mech Sci 99 (2015), 21–8. https://doi.org/https://doi.org/10.1016/j.ijmecsci.2015.05.007

[5] K Yoshida, T Kuwabara, M Kuroda, Path-dependence of the forming limit stresses in a sheet metal, Int J Plast 23 (2007) 361–84. https://doi.org/https://doi.org/10.1016/j.ijplas.2006.05.005

[6] K Yoshida, T Kuwabara, Effect of strain hardening behavior on forming limit stresses of steel tube subjected to nonproportional loading paths, Int J Plast 23 (2007), 1260–84. https://doi.org/https://doi.org/10.1016/j.ijplas.2006.11.008

[7] TO Erinosho, ACF Cocks, FPE Dunne, Coupled effects of texture, hardening and non-proportionality of strain on ductility in ferritic steel, Comput Mater Sci 80 (2013) 113–22. https://doi.org/https://doi.org/10.1016/j.commatsci.2013.03.002.

[8] TO Erinosho, ACF Cocks, FPE Dunne, Texture, hardening and non-proportionality of strain in BCC polycrystal deformation, Int J Plast 50 (2013) 170–92. https://doi.org/https://doi.org/10.1016/j.ijplas.2013.04.008

[9] H Ghadbeigi, C Pinna, S Celotto, JR Yates, Local plastic strain evolution in a high strength dual-phase steel, Mater Sci Eng A 527 (2010) 5026–32. https://doi.org/https://doi.org/10.1016/j.msea.2010.04.052

[10] S Celotto, H Ghadbeigi, C Pinna, BA Shollock, P Efthymiadis, Deformation-Induced Microstructural Banding in TRIP Steels, Metall Mater Trans A 49 (2018) 2893–906. https://doi.org/10.1007/s11661-018-4650-z.

[11] C Caër, R Pesci, Local behavior of an AISI 304 stainless steel submitted to in situ biaxial loading in SEM, Mater Sci Eng A 690 (2017) 44–51. https://doi.org/https://doi.org/10.1016/j.msea.2017.02.087

[12] GOM, GOM ARAMIS. 2009. https://www.gom.com/metrology-systems/aramis (Accessed 27-03-2020)

[13] NS Small, SK Hazra, DK Williams, R Roy, Measuring and representing the formability of sheet materials in the presence of heterogeneous plastic deformation, Int. J of Adv Mat Tech 109 (2020) 397-410. https://doi.org/10.1007/s00170-020-05372-0

[14] LaVision, DaVis Strain Master Software, DaVis 10. 2017. https://www.lavision.de/en/products/davis-software/ (Accessed 26-09-2021)